

PAPER • OPEN ACCESS

# Study of Thermomechanical Properties of The Epoxy-Impregnated Cable Composite for a 15 T Nb<sub>3</sub>Sn Dipole Demonstrator

To cite this article: Pei Li *et al* 2017 *IOP Conf. Ser.: Mater. Sci. Eng.* **279** 012020

View the [article online](#) for updates and enhancements.

## Related content

- [Cable deformation simulation and a hierarchical framework for Nb<sub>3</sub>Sn Rutherford cables](#)  
D Arbelaez, S O Prestemon, P Ferracin et al.
- [Measurement of a Conduction Cooled Nb<sub>3</sub>Sn Racetrack Coil](#)  
HS Kim, C Kovacs, J Rochester et al.
- [Irreversible degradation of Nb<sub>3</sub>Sn Rutherford cables due to transverse compressive stress at room temperature](#)  
Patrick Ebermann, Johannes Bernardi, Jerome Fleiter et al.

# Study of Thermomechanical Properties of The Epoxy-Impregnated Cable Composite for a 15 T Nb<sub>3</sub>Sn Dipole Demonstrator

Pei Li, Steve Krave, Alexander Zlobin

Fermi National Accelerator Laboratory, Batavia, IL, 60510

peili@fnal.gov

**Abstract.** The knowledge of the thermomechanical properties of the composite of cable/insulation/epoxy impregnation are important for the design, fabrication and operation of superconducting accelerator magnets. As a part of the 15 T dipole magnet development at Fermi National Accelerator Laboratory (FNAL), we studied the thermomechanical properties of cable stack that represents the cable composites in the 15 T dipole. The measurements include thermal contraction and strain-stress characterization under compressive load along the principal directions. The cable stack samples show hysteresis behaviour in loading-unloading cycles, which is found to be most dramatic along the azimuthal direction. Also, the choice of insulation material/procedure is found to strongly impact the bonding between cables and epoxy/cable layers. The cable stacks measured in this study use E-glass tape wrapping insulation and show weaker bonding to cables than similar cable stacks using S-2 glass sleeves insulation previously studied.

## 1. Introduction

Superconducting magnets that generate 15 T field is crucial to the realization of hadron collider with energy level beyond that of LHC. Fermi National Accelerator Laboratory (FNAL) started the development of a 15 T Nb<sub>3</sub>Sn dipole demonstrator magnet based on the “cosine theta” design [1-3].

In the development of the 15 T dipole, the knowledge of the thermomechanical properties of all the components are very important. The supporting structures of the magnet are fabricated from metals and their thermomechanical properties are well known. On the other hand, the cable composite (Nb<sub>3</sub>Sn cable/insulation/epoxy impregnation) is more complicated because it contains several components of drastically different thermomechanical properties and its fabrication is a multiple-variable procedure which can result in significant variation of properties. To provide reliable and relevant thermomechanical properties data to the design and fabrication of magnets, it is important to perform measurements on samples that best represent the cable composite used in the magnets.

## 2. Sample Description

The thermomechanical properties measurements were performed on cable stacks that were fabricated using the same technology and materials as in the 15 T dipole. Specifically, the cable studied here is used to wind the two outer layers of the dipole [1]. The detailed information of the cable and insulation is shown in table 1.



**Table 1.** Specification of the cable stacks

Specification	
Nb <sub>3</sub> Sn strand	0.7 mm 108/127 RRP strand
cable	40 strands, with core
insulation	E-glass tape wrapping, 0.075 mm thick, 12.7 mm wide
Binder	CTD1202X, cured for 120 °C/30 min in air
Reaction procedure	210 °C/48 h, 400 °C/48 h, 640 °C/48 h, in flowing Ar
Epoxy impregnation	CTD101K

To prepare the cable stack sample, the cable was cut into 6.5 inch long pieces. After cutting, the ends of the cable pieces were sealed by tungsten inertia gas (TIG) welding to prevent the leakage of tin during heat treatment. A 0.075 mm thick, 12.7 mm wide E-glass insulation tape was wrapped around the cable pieces, with a 40-50% turn-to-turn overlap. 10 wrapped cable pieces were stacked in a reaction fixture, with alternating the wide and the narrow edges. A ceramic binder CTD1202X was uniformly brushed over the stacked cables. The reaction fixture was first heated in air at 120 °C for 30 minutes to cure the binder and then reacted in a tube furnace (210 °C 48 hrs/400 °C 48 hrs/640 °C 48 hrs) in flowing Ar gas. The reacted cable stack was impregnated using CTD101K epoxy. Each impregnated cable stack has a usable length of 6 inch and a cross section of 15.6 mm by 17.2 mm. A full cable stack was further cut into shorter (0.6-2 inches) segments for measurements using a low-speed diamond saw. A cable stack sample has three principal directions, *i.e.* azimuthal, radial and axial, as illustrated in figure 1.

The deformation of samples was measured with strain gages (type WK350-13-125AD-W by MicroMeasurement) and the gage installations were performed following the standard procedure using M-bond (type AE10).

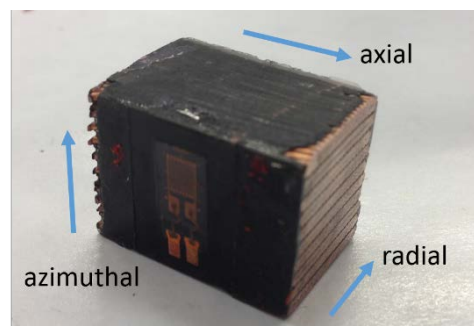


**Figure 1.** A cable stack sample with the three principal orthogonal directions labeled. On this sample, a gage is installed to measure the azimuthal strain.

### 3. Thermal Contraction Measurement

To measure the thermal contraction of cable stacks, gages were mounted along the principal directions. The samples were gradually cooled from room temperature (~293 K) to 77 K over 30 minutes and the change of gage resistance,  $\Delta R$ , was measured.

The measured  $\Delta R$  includes: (i) the resistance change of gage material with temperature; (ii) resistance change proportional to the thermal contraction difference between the gage grid alloy and the tested

material. To extract the thermal contraction of the sample, a material with known thermal contraction should be measured with the same type of strain gage as reference [4]. We used high-purity quartz as the reference material, of which the thermal contraction was taken to be zero. As verification, we also measured a piece of Al-6061 and the thermal contraction from 293 K to 77 K is 0.37%, comparing with the theoretical value of 0.389%. The thermal contraction results of the cable stacks are listed in table 2.

**Table 2.** Thermal contraction results

Sample	Thermal contraction (%), 293 K to 77 K
Cable stack, radial	0.436
Cable stack, azimuthal	0.19
Cable stack, axial	0.215
Al-6061	0.37
Al-6061 (calculated)	0.389

#### 4. Mechanical Property Measurements

The strain-stress curves of cable stacks were tested under compression along its principal orthogonal directions in a calibrated hydraulic loader at room temperature. The samples were compressed in stainless steel fixtures. The strain of the samples was measured by strain gages. Each test included three loading-unloading cycles between zero and the pre-set peak load. A typical strain-stress curve from a piece of Al-6061 is shown in figure 2. Above 5 MPa, the strain-stress curve is linear and the fitted Young's modulus is 71.2 GPa, comparing with the typically reported value of about 70 GPa.

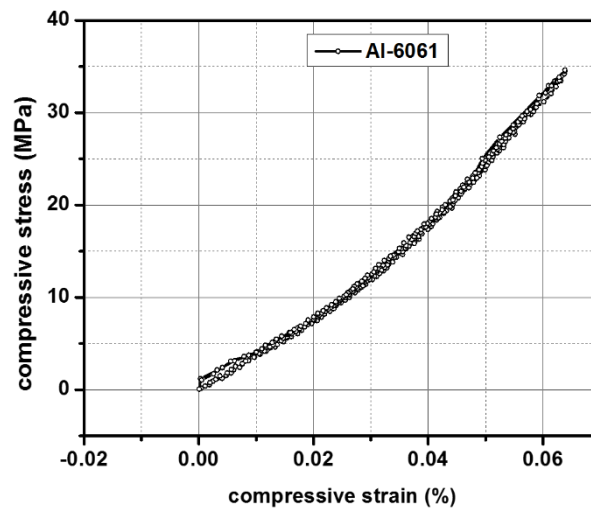


**Figure 2.** The strain-stress curve of a piece of Al-6061 sample. Three loading-unloading cycles are shown.

##### 4.1. Strain-stress characterization of cable stacks under azimuthal load

The strain-stress curves of cable stacks under azimuthal load are shown in figure 3. Figure 3(A) shows the results of the initial, low-level azimuthal loading of a sample. As described above, three cycles between zero and the peak load (~11 MPa) were performed. At the end of the first loading-unloading cycle, with zero stress, the sample is under ~0.005% compressive strain. This shows that an azimuthal load of ~11 MPa already induces plastic deformation in the sample. Also, we notice that in the subsequent two cycles, the sample shows hysteresis behaviour. The loading curves (of the second and

the third cycle) and the unloading curves (of all the three cycles) follow two different traces. On the other hand, these cycles do not further increase the plastic deformation in the sample. Fitting of these curves shows the Young's modulus along the azimuthal direction to be  $\sim 17$  GPa. Figure 3(B) shows the results of gradually increasing the peak azimuthal load. The residual plastic deformation increases with the peak load. With a peak load of 140 MPa, the plastic deformation is about 0.75%. These cycles also show similar hysteresis behaviour observed in the low-level loading tests.

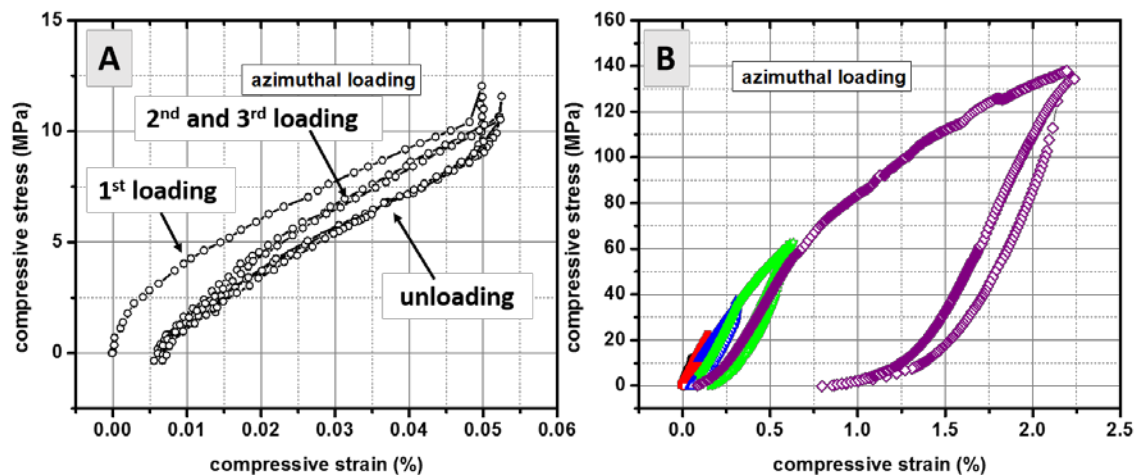


**Figure 3.** Strain-Stress curves of cable stack under azimuthal load. (A) The initial three loading-unloading cycles up to 11 MPa. (B) Cyclical loading with increasing the peak load to 11, 20, 40, 60 and 140 MPa respectively.

#### 4.2. Strain-stress characterization of cable stacks under radial load

The strain-stress curves of cable stacks under radial load are shown in figure 4. Figure 4(A) shows the results of the initial radial loading of a sample to a peak load of  $\sim 11$  MPa. After three cycles, the sample shows no plastic deformation and the hysteresis between loading and unloading curves are less significant comparing with azimuthal loading. The fitted Young's modulus is about 49.2 GPa. Figure shows the results of increasing the peak load. With increasing the peak load, the sample begins to show plastic deformation and the hysteresis behaviour becomes more obvious. To date, we have completed radial loading-unloading cycles up to 35 MPa and the residual plastic deformation is about 0.01%.

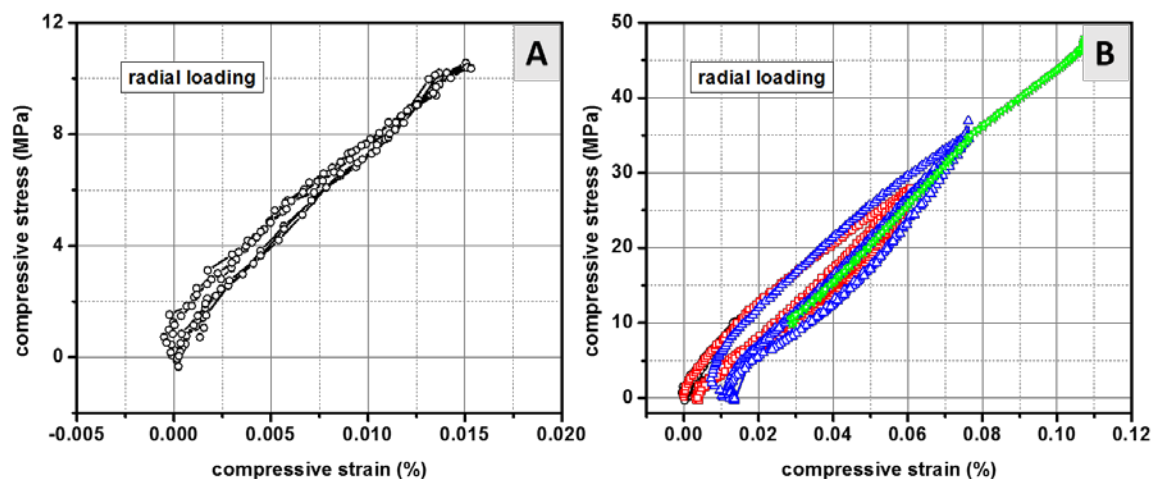


**Figure 4.** Strain-stress curves of cable stack under radial load. (A) the initial three loading-unloading cycles of a sample up to 11 MPa. (B) Cyclical loading of the sample with increasing peak load.

With further increasing the peak radial load, we observed sample failure. An example is shown in figure 5. As shown by the strain-stress curve, when load reaches about 50 MPa, the compressive strain measured by the gage suddenly begins to drop and continues to decrease until the peak load of ~ 62 MPa. During unloading, the measured strain remains constant around -0.03%. Since compressive strain is considered positive here, a negative value indicates tensile strain. After the removal of the sample from the test fixture, we found bulging of the sample, with the outmost of the layers bent outward and partially delaminated from the stack. Since the strain gage is mounted on the sample surface, the observed drop of compressive strain during loading and the residual tensile strain is because of the local deformation of the outmost layers.

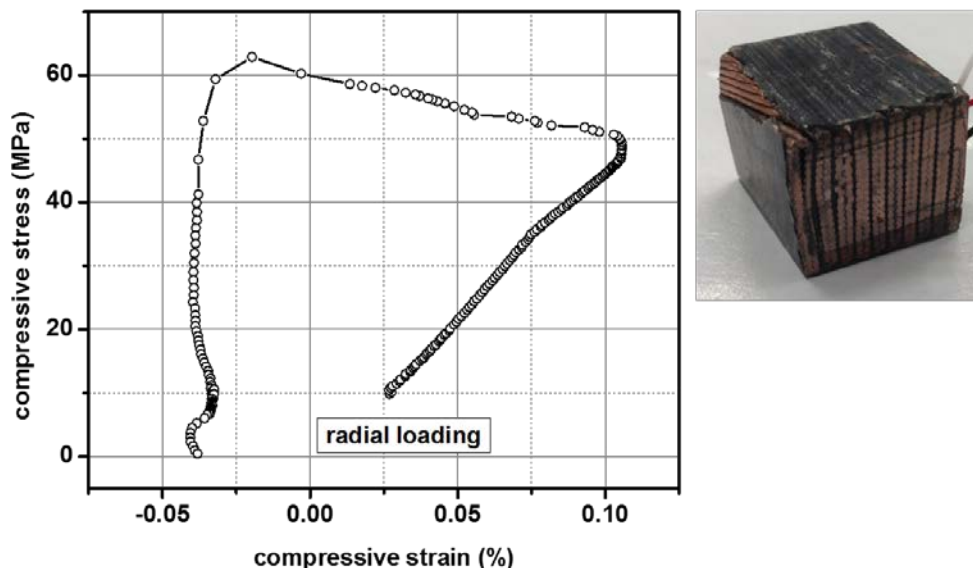


**Figure 5.** The failure of a sample during radial loading. Left, the strain-stress curve. The sample failure occurred at ~ 50 MPa and further loading caused the measured strain to drop to ~-0.03%, which remained constant during unloading. Right, photo of the sample after loading test. Bulging of the sample and the delamination of the outmost layers were found. See the text for more details.

## 5. Discussion

In compressive loading tests, the cable stacks show clear hysteresis between loading and unloading. In contrast, the loading and unloading curves of Al-6061, an elastic material, overlap well. This suggests that in the design and modelling of magnets, the cable composites should not be treated as purely elastic. In the operation of magnet, when the strain status of a magnet changes, hysteresis leads to energy dissipation, which may contribute to magnet instability.

E-glass has been chosen as an insulation material because of its low cost and availability [5] and has been adopted by other magnets. While various properties of E-glass insulation have been investigated, including thermal conductivity, thermal contraction [6] and dielectric strength [5], the strain-stress characterization properties of cable composites using E-glass has not been intensively studied yet. The similar studies so far have been focused on composites using S-2 glass and ceramic insulation [4]. This is the first time Nb<sub>3</sub>Sncable stacks using this insulation method (E-glass tape wrapping and binder) was systematically measured for their thermomechanical properties. During the fabrication and the handling of the cable-stack samples with E-glass insulation, we noticed that the bonding between cable and

epoxy/insulation layer is weaker than similar samples with S-2 glass insulation. While the load tests of control samples with S-2 glass are in progress, in a recent study on similar cable stacks with S-2 glass sleeve insulation [7], where the test condition is similar to this work, radial load was successfully applied beyond 100 MPa without sample failure. In contrast, we found that 50 MPa radial load can cause delamination in our cable stacks using E-glass wrapping insulation. On the other hand, the test method used does not fully represent the stress condition of the cable composite in real magnets. The loading fixture does not provide constraints to sample surfaces that are parallel to load whereas the cable composite is constrained by the mechanical structure in magnets. To extend the tests into high stress (> 200 MPa) regime, which is of more interest to the development of high field magnets, loading fixtures that provide mechanical constraints should be used.

## 6. Conclusion

Thermal contraction and strain-stress characterization were performed on cable stacks that represents the cable composite in the 15 T dipole magnet being developed at FNAL. The cable stacks show hysteresis behaviour in loading-unloading cycles. The bonding to cables of E-glass wrapping insulation is found to be weaker than S-2 glass sleeve insulation previously studied, which leads to early delamination in samples compressed without mechanical constraints at 50 MPa radial load. We will extend tests in high stress regime (> 200 MPa) regime with improved test fixture and samples fabricated from the inner layer cables of the 15 T dipole (28 1.0 mm strands) as well as control samples with S-2 glass will be included.

## References

- [1] Andreev N, Barzi E, Carmichael J, Kashikhin V, Novitski I, Turrinoni D and Zlobin A, *Fermilab technical report*, TD-16-004.
- [2] Kashikhin V, Andreev N, Barzi B, Novitski I and Zlobin A, *IOP Conf. Series: Materials Science and Engineering* 101 (2015) 012055 .
- [3] Novitski I, Andreev N, Barzi E, Carmichael J, Kashikhin V, Turrioni D, Yu M and Zlobin A, *IEEE Trans. Appl. Supercond.* 26(4):1 2016
- [4] Chichili D, Arkan T, Ozelis J and Terechkin I, *IEEE Trans. Appl. Supercond.* 10(1):1317 2000
- [5] Bossert R, Ambrosio G, Andreev N, Whitson G and Zlobin A, *AIP Conf. Proc.* 986:161 2008
- [6] Imbasciati L, Volpini G, Ambrosio G, Chichili D, Pedrini D, Previtali V, Rossi L and Zlobin A, *IEEE Trans. Appl. Supercond.* 13(2):1788 2003
- [7] Bossert R, Krave S, Ambrosio G, Andreev N, Chlachidze G, Nobrega A, Novitski I, Yu M and Zlobin A, *AIP Conf. Proc.* 1574:132 2014